Global Biogeochemical Cycles

RESEARCH ARTICLE
10.1029/2020GB006626

Long-Term Shifts in U.S. Nitrogen Sources and Sinks Revealed by the New TREND-Nitrogen Data Set (1930–2017)

D. K. Byrnes[1], K. J. Van Meter[2], and N. B. Basu[1,3,4]

[1]Department of Civil and Environmental Engineering, University of Waterloo, Waterloo, ON, Canada, [2]Department of Earth and Environmental Sciences, University of Illinois at Chicago, Chicago, IL, USA, [3]Department of Earth and Environmental Sciences, University of Waterloo, Waterloo, ON, Canada, [4]Water Institute, University of Waterloo, Waterloo, ON, Canada

Key Points:
- A county-scale data set for components of the nitrogen (N) mass balance (TREND-nitrogen) was developed for the contiguous United States, 1930–2017
- Cluster analysis was used to identify 10 clusters with unique N surplus trajectories
- Similar nitrogen trajectories across diverse geographic regions indicate widespread functional homogenization of human-dominated landscapes

Supporting Information:
- Supporting Information S1

Correspondence to:
N. B. Basu,
nandita.basu@uwaterloo.ca

Citation:
Byrnes, D. K., Van Meter, K. J., & Basu, N. B. (2020). Long-term shifts in U.S. nitrogen sources and sinks revealed by the new TREND-nitrogen data set (1930–2017). *Global Biogeochemical Cycles*, *34*, e2020GB006626. https://doi.org/10.1029/2020GB006626

Received 6 APR 2020
Accepted 20 AUG 2020
Accepted article online 24 AUG 2020
Corrected 24 FEB 2022

This article was corrected on 24 FEB 2022. See the end of the full text for details. All corrections have been made to the online version.

Abstract Reactive nitrogen (N) fluxes have increased tenfold over the last century, driven by increases in population, shifting diets, and increased use of commercial N fertilizers. Runoff of excess N from intensively managed landscapes threatens drinking water quality and disrupts aquatic ecosystems. Excess N is also a major source of greenhouse gas emissions from agricultural soils. While N emissions from agricultural landscapes are known to originate from not only current-year N input but also legacy N accumulation in soils and groundwater, there has been limited access to fine-scale, long-term data regarding N inputs and outputs over decades of intensive agricultural land use. In the present work, we synthesize population, agricultural, and atmospheric deposition data to develop a comprehensive, 88-year (1930–2017) data set of county-scale components of the N mass balance across the contiguous United States (Trajectories Nutrient Dataset for nitrogen [TREND-nitrogen]). Using a machine-learning algorithm, we also develop spatially explicit typologies for components of the N mass balance. Our results indicate a large range of N trajectory behaviors across the United States due to differences in land use and management and particularly due to the very different drivers of N dynamics in densely populated urban areas compared with intensively managed agricultural zones. Our analysis of N trajectories also demonstrates a widespread functional homogenization of agricultural landscapes. This newly developed typology of N trajectories improves our understanding of long-term N dynamics, and the underlying data set provides a powerful tool for modeling the impacts of legacy N on past, present, and future water quality.

Plain Language Summary Over the last century, people have increasingly used nitrogen fertilizer to increase crop yields. The nitrogen not taken up by crops in agricultural areas runs off of the land and pollutes rivers, lakes, and coastal areas. This excess nitrogen also forms a powerful greenhouse gas that contributes to climate change. Excess nitrogen can build up in the environment over time and pollute our water for decades. It is therefore necessary for us to know how much extra nitrogen has been applied over many decades to better understand current risks to the environment. In our study, we have used multiple data sources to calculate how much nitrogen has been added to the landscape, how much nitrogen has been removed through crop production, and how much human waste is produced, for every county in the contiguous United States from 1930 to 2017. We show that the main sources of nitrogen can be different in different areas of the country. We also show that high levels of nitrogen use can make landscapes in very different climates look very similar. This new data set will be very important for creating models that can predict how decades of high nitrogen inputs impact water quality and future changes in climate.

1. Introduction

Worldwide increases in the fluxes of reactive nitrogen (N) threaten drinking water quality, disrupt aquatic ecosystems, and escalate emissions of greenhouse gases (Camargo & Alonso, 2006). In the United States, 7% of domestic wells have been found to exceed the 10 mg N L^{-1} drinking water standard for nitrate (Dubrovsky et al., 2010), and recent work suggests that human health is negatively impacted even at concentrations as low as 0.9 mg N L^{-1} (Schullehner et al., 2018; Ward et al., 2018). In Denmark, more than 40% of monitoring wells are reported to have concentrations greater than the WHO drinking water standard (Hansen et al., 2017), and in China, it has been suggested that at least 28% of wells exceed this standard

(Gu et al., 2013). In coastal regions, we see N-driven increases in the incidence of harmful algal blooms (HABs) and the development of large dead zones. Problems of nutrient-induced hypoxia have been noted for decades along the Louisiana continental shelf in the Gulf of Mexico and in the Chesapeake Bay (Harding et al., 2019; Rabalais et al., 2002; Van Meter et al., 2017). Excess N in soils and surface water also leads to increased GHG emissions, with agriculture accounting for approximately 63% of all anthropogenic emissions of N_2O (Syakila & Kroeze, 2011).

At both global and local scales, increased N fluxes are dominated by the food and energy requirements of a growing human population. Development of the Haber-Bosch process for fixing atmospheric N paved the way for industrial-scale production of commercial N fertilizers (Smil, 1999). Increased fertilizer use fueled a post-WW2 revolution in farming and a doubling and tripling of crop yields (Mosier et al., 2004). Increasing population, differences in dietary choices, and changes in energy policy have led to increased meat consumption, increases in livestock grain requirements, rising corn-based ethanol production, and increases in the agricultural land area necessary to maintain desired production levels (Alexander et al., 2015; Donner et al., 2004; Hudiburg et al., 2016). As livestock feeding operations have been more concentrated, overapplication of excess manure N to crop and pastureland has become commonplace (Metson et al., 2016).

Increasingly, efforts are being made to quantify the nature and magnitude of changes in anthropogenic N cycling. It has been estimated that more than 150 Tg of anthropogenic, reactive N is added to the global N cycle each year through industrial fixation processes, cultivation of N-fixing crops, and the burning of both fossil fuels and biomass, and some suggest that this human intensification of the global N cycle has transgressed planetary boundaries (Galloway et al., 2008; Rockström et al., 2009). At a country scale, it has been shown that more than 50% of anthropogenic N is lost to the environment, with losses varying as a function of climate, crop type, and fertilizer application rates (Lassaletta et al., 2014).

There have been many attempts to bring both mass balance and process-based modeling approaches to considerations of water quality in intensively managed watersheds. Such attempts have ranged from simple input-output N budgets (Goyette et al., 2016; Hong et al., 2011, 2012; Kopáček et al., 2013; Swaney et al., 2018) to complex biogeochemical process models (Del Grosso et al., 2002; Ilampooranan et al., 2019; Yiridoe et al., 1997). The first category is the Net Anthropogenic Nitrogen Inputs (NANI) approach, which calculates the difference between all anthropogenic inputs and outputs (atmospheric deposition, commercial N fertilizer application, crop N fixation, N inputs and outputs of food and feed) to a watershed (Hong et al., 2011). Based on this approach, significant linear relationships have been noted between net N inputs to a watershed and measured fluxes of riverine N, with some suggesting that approximately 25% of net N inputs are lost to downstream waters (Boyer et al., 2002; Howarth et al., 2006; Swaney et al., 2012). Adding more complexity, empirical models such as SPARROW (R. B. Alexander et al., 2001), GREEN (Grizzetti et al., 2005), and NEWS (Mayorga et al., 2010) have been used to predict riverine N loads based on a function of watershed N inputs and terrestrial and aquatic retention factors that are calibrated to nitrogen loads at the watershed outlet. Finally, more sophisticated biogeochemical models, such as DAYCENT, CENTURY, and SWAT, explicitly simulate various N fluxes (e.g., denitrification and crop uptake leaching) using detailed process-based equations (Del Grosso et al., 2002; Ilampooranan et al., 2019; Yiridoe et al., 1997).

The above approaches make one critical assumption that may limit their real-world accuracy: that a given year's N balance is the primary driver of that year's N fluxes. Indeed, it is increasingly understood that N emissions from agricultural landscapes are a function not only of current-year N inputs but also of legacy N that may have accumulated over decades of fertilizer application and intensive livestock production (Ascott et al., 2017; Chen et al., 2014; Sebilo et al., 2013; Van Meter et al., 2016). For example, studies of nitrate pollution in the U.S. Mississippi River Basin suggest that as much as 85% of the current riverine N load is made up of legacy N (Van Meter et al., 2017, 2018).

Therefore, to better understand long-term N dynamics, and in particular, the role of N legacies in driving both dissolved and gaseous emissions of N from human-impacted landscapes, it is crucial to develop long-term data sets of N inputs and outputs. In their analysis of Mississippi and Susquehanna River Basin trends in riverine nitrate, Van Meter et al. (2017) developed such a data set, allowing them to estimate watershed-scale N balances from 1800 to 2016. Their estimates, however, were based on state-level Agricultural Survey data, thus limiting the spatial resolution of their results. To provide finer spatial resolution, Swaney et al. (2018) have developed a county-scale data set of anthropogenic N inputs and outputs

covering much of the contiguous United States, and Sabo et al. (2019) have built upon this work to provide more complete geographic coverage and a more inclusive inventory of N inputs. In addition, Hamlin et al. (2020) have developed estimates of landscape N inputs across the Great Lakes region at a 30-m spatial resolution. All of these data sets, however, are limited in their temporal extent. The Swaney et al. (2018) data set provides N inputs and outputs at 5-year intervals for the period 1987–2012, the Sabo et al. (2019) data set covers only the years 2002, 2007, and 2012, and the Hamlin et al. (2020) data set only the years 2008–2015. To provide greater temporal coverage, Yang et al. (2016) have developed a county-scale data set covering the period 1930–2012, but their data are limited to manure nutrient production.

Here, we address these limitations by constructing a long-term (1930–2017), county-scale N mass budget for the contiguous United States—the Trajectories Nutrient Dataset for nitrogen (TREND-nitrogen). In this work, we quantify individual components of the anthropogenic N balance and also calculate county-scale, N surplus magnitudes, which we define here as a simple sum of N inputs (fertilizer N application, biological N fixation, atmospheric N deposition, manure N, and human waste) and nonhydrologic outputs (crop N uptake). In carrying out this work, our primary objectives were to (1) provide multidecadal, fine-scale, trajectories of N inputs and outputs across the contiguous United States and (2) to investigate spatial and temporal changes in the county-scale patterns in N inputs and outputs in the context of historical changes in population, land use, and management.

2. Materials and Methods

Details regarding compilation of the mass balance data set are provided in section 2.1. Additional methods related to our cluster analysis and development of the N surplus typologies are provided in section 2.2.

2.1. Data Set Preparation: The Nitrogen Mass Balance

Components of the N mass balance were calculated for the period 1930–2017 at a county scale across the contiguous United States. All data related to this mass balance are included in the TREND-nitrogen data set (https://doi.org/10.1594/PANGAEA.917583) (Byrnes et al., 2020). Details regarding the calculation of individual components of the mass balance are provided below and in the Supporting Information S1. For a summary of the individual components and related data sources, see Table S1.

Note that compilation of such a large data set requires the use of many different underlying data sets, often compiled by different organizations, at different scales, for different reasons. The harmonization of such data sets not only presents methodological challenges but also provides substantial benefits, in this case in the form allowing large-scale comparisons of N dynamics across spatial and temporal scales. Specific challenges related to this harmonization are addressed in the sections below related to individual components of the mass balance.

2.1.1. Atmospheric N Deposition

Atmospheric N deposition, *DEP*, was calculated as the sum of wet and dry deposition of oxidized forms of N (NO_x). Three primary data sets were used to calculate N deposition over the 1930–2017 study period: (1) U.S. 4 km × 4 km gridded wet (1986–2017) and dry (2000–2017) deposition data (National Atmospheric Deposition Program, 2018); (2) national NO_x emission trend data (1943–2008) (Houlton et al., 2013); and (3) global 450 km × 420 km gridded deposition data (1860–2050) (Dentener, 2006). For additional details regarding development of the 1930–2017 deposition data set, see Text S1.1.

2.1.2. N Fertilizer

County-scale estimates of N fertilizer use (domestic and agricultural), *FERT*, were obtained for the period 1945–1985 from Alexander and Smith (1990) and for the period 1987–2012 from Brakebill and Gronberg (2017). For the period 1930–1944, we used gridded, 5 km × 5 km resolution, estimates of N fertilizer application from Cao et al. (2018). For the period 2012–2017, we estimated county-scale N fertilizer inputs based on national fertilizer use data (1994–2017), which we scaled to individual counties based on established ratios of county to national-scale use for the period 2008–2012 (USDA, 2018). For additional details regarding development of the 1930–2017 fertilizer data set, see Text S1.2.

2.1.3. Biological N Fixation

Biological N fixation, *BNF*, the process by which nonreactive atmospheric N is microbially fixed and converted to reactive N (Galloway et al., 1995), was calculated for cropland using area- and yield-based methods (Bouwman et al., 2005; Han & Allan, 2008; Hong et al., 2013). BNF input values were calculated for the

following crops: soybeans, peanuts, lentils, dry beans, snap beans, hay (alfalfa and non-alfalfa), and cropland pasture. Calculations were based on county-scale estimates of cropped area and crop production data obtained from the U.S. Agricultural Census. Data for census years between 1930 and 2012 were obtained from a digitized Agricultural Census data set housed within the Inter-university Consortium for Political and Social Research (ICPSR) data archive (Haines et al., 2018). Data for the 2017 census year were obtained through the USDA National Agricultural Statistics Service (NASS) Quick Stats tool (USDA NASS, 2017). For additional details and parameters used in the calculations, see Text S1.3 and Tables S2 and S3.

2.1.4. Manure N Inputs

Manure N inputs, *MAN,* which we define here as all waste excretion from livestock production, were estimated using livestock inventory data available through the U.S. Agricultural Census. Data were obtained from the ICPSR data archive (1930–2012) (Haines et al., 2018) and NASS Quick Stats. Eleven different livestock categories (dairy cattle, beef cattle, heifers, steers, chickens, pullets, broilers, turkeys, hogs, sheep, and horses) were included in the calculations, similar to other studies (Boyer et al., 2002; Goyette et al., 2016; Hong et al., 2011; Yang et al., 2016). These 11 categories were confirmed to contribute over 95% of all manure produced in each state based on 2012 livestock inventory estimates. Manure N was calculated using the product of reported heads of livestock and the annual N content of the manure generated per animal and then normalized by county area (kg N ha^{-1} y^{-1}). For additional details and parameters used in the calculations, see Text S1.4 and Tables S4 and S5.

2.1.5. Crop N Uptake

Crop N uptake, CROP, was calculated using county-scale, crop-specific production data from the Agricultural Census. Data were obtained from the ICPSR data archive (1930–2012) (Haines et al., 2018) and NASS Quick Stats (2017) (USDA-NASS, 2017). A total of 63 different crops, including field crops, fruit and nut trees, fruits, and vegetables, were used in calculating this component of the N budget. This selection of crops, which was confirmed to cover ≥97% of the county-scale cropped area (USDA NASS Cropland Data Layer, 2010), is much broader than that accounted for in other studies. For example, Swaney and Howarth (2019) include only 16 crop types for N uptake calculations, and Sabo et al. (2019) explicitly include 21 crop types, plus an "other crop" category for which uptake was calculated using a mean N uptake parameter. Parameter values used to convert crop production data to crop N uptake values (kg N ha^{-1} y^{-1}) in the present study are given in Table S6, and for additional details regarding the calculation of the crop N uptake values, see Text S1.5 and Table S6).

2.1.6. Human N Waste Inputs

Inputs of N associated with human waste, *HUM*, were estimated using population census data and literature estimates of per capita human annual N excretion (5 kg N y^{-1}) (Hong et al., 2011). Decadal county-scale population census data were available from 1930 to 1990 (U.S. Census Bureau, 2007), and annual data were available after 1990 (U.S. Census Bureau, 2016). For the period 1930–1990, we interpolated decadal census data to obtain annual estimates of population. County-scale human N waste inputs were calculated as the product of the N excretion rates and county-scale population numbers. Note that a significant fraction of this waste is treated in wastewater treatment plants or septic systems before it is discharged to the environment. The treatment efficiencies of human waste vary spatially and also have changed significantly over the last 88 years. Developing these trajectories is beyond the scope of the current work.

2.1.7. N Surplus Calculation

We define the county-scale N surplus, NS_{cnty} (kg N ha^{-1} y^{-1}), as the difference between N inputs (atmospheric N deposition, fertilizer N, manure N, biological N fixation, and human N waste) and "productive" N outputs (crop and pastureland N uptake) (Bouwman et al., 2005; Hong et al., 2013; Van Meter et al., 2017) (Figure 1 and Equation 1).

$$NS_{cnty} = DEP + FERT + BNF + MAN + HUM - CROP \quad (1)$$

where *DEP* is atmospheric N deposition (kg N ha^{-1} y^{-1}); *FERT* is inorganic N fertilizer (kg N ha^{-1} y^{-1}); *BNF* is biological N fixation in legume crops (kg N ha^{-1} y^{-1}); *MAN* is N in livestock waste (kg N ha^{-1} y^{-1}); *HUM* (kg N ha^{-1} y^{-1}) is N in human waste; *CROP* represents crop N uptake and N consumption by grazing livestock (kg N ha^{-1} y^{-1}). NS_{cnty} magnitudes are reported as median values along with their interquartile range (IQR).

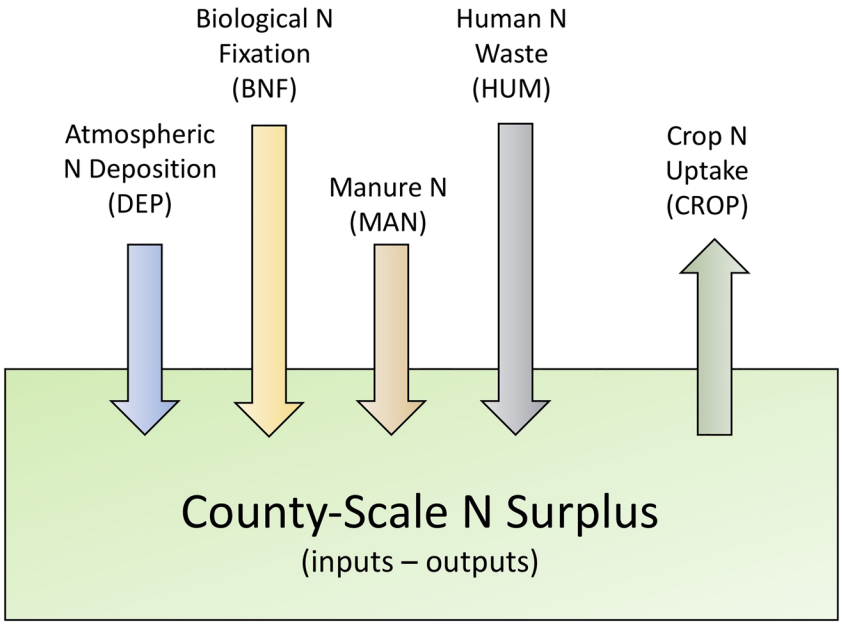

Figure 1. Conceptual diagram showing fluxes associated with major components of the N mass balance. The county-scale N surplus, NS_{cnty}, is calculated, using the TREND-nitrogen data set, as the difference between N inputs (atmospheric N deposition, biological N fixation, manure N, and human N waste) and N outputs in the form of crop harvest and consumption of pastureland grasses by grazing livestock.

The NS_{cnty} N surplus metric used herein includes only nonhydrologic outputs. As discussed by Sabo et al. (2019) with regard to their 2002–2012 U.S. N mass balance, the surplus N is considered to have three possible fates: (1) storage within the landscape, in soils or groundwater; (2) losses to the atmosphere due to denitrification; or (3) export from the landscape as riverine N. Storage and denitrification magnitudes are not included here due to difficulties in estimation and a lack of reliable data at appropriate scales. Riverine N magnitudes are not specified herein, as these estimates must be made at a watershed scale. The developed data sets will be useful to include in landscape and watershed-scale modeling efforts, which, in the future, can be used to better quantify currently unspecified N fates.

2.2. Clustering of N Mass Balance Trajectories

We used *k*-means cluster analysis to (1) identify clusters of counties across the contiguous with similar trajectories for individual components of the N mass balance (*FERT*, *BNF*, *MAN*, *DEP*, *HUM*, *CROP*) and (2) identify clusters of counties with similar N surplus trajectories. The *k*-means algorithm is an unsupervised learning algorithm that minimizes the sum of squared error among a specified number of groups, using an iterative approach (Hartigan & Wong, 1979; Likas et al., 2003). One cluster center is added at a time, with *N* executions of the *k*-means algorithm, where *N* is the size of the data set (Likas et al., 2003). The algorithm is initiated with *k* initial seeds for the clusters, and all *N* data are compared with each seed (Ay & Kisi, 2014). The intracluster variance is iteratively minimized by minimizing the sum of squared Euclidean distances (EDs) (MacKay & Mac, 2003). We carried out the analysis using the Matlab Statistics and Machine Learning Toolbox (Mathworks, R2018b).

2.2.1. Individual Component Clusters

To identify clusters for individual components of the mass balance, we divided the 88-year study period into five periods: 1930–1940, 1941–1960, 1961–1980, 1981–2000, and 2001–2017. For each period, we calculated (1) the mean annual value (kg N ha^{-1} y^{-1}) for that component and (2) the linear slope for the component trajectory, giving us a total of 10 metrics, or features, for each county to use with the *k*-means algorithm.

For each analysis, the *k*-means algorithm was run for a range of *k* values, and the ED value was plotted against the number of clusters for each run. The optimal number of clusters was then selected using the "Elbow Method", which is based on visual inspection of a plot of ED values versus *k*, with the "elbow" *k*

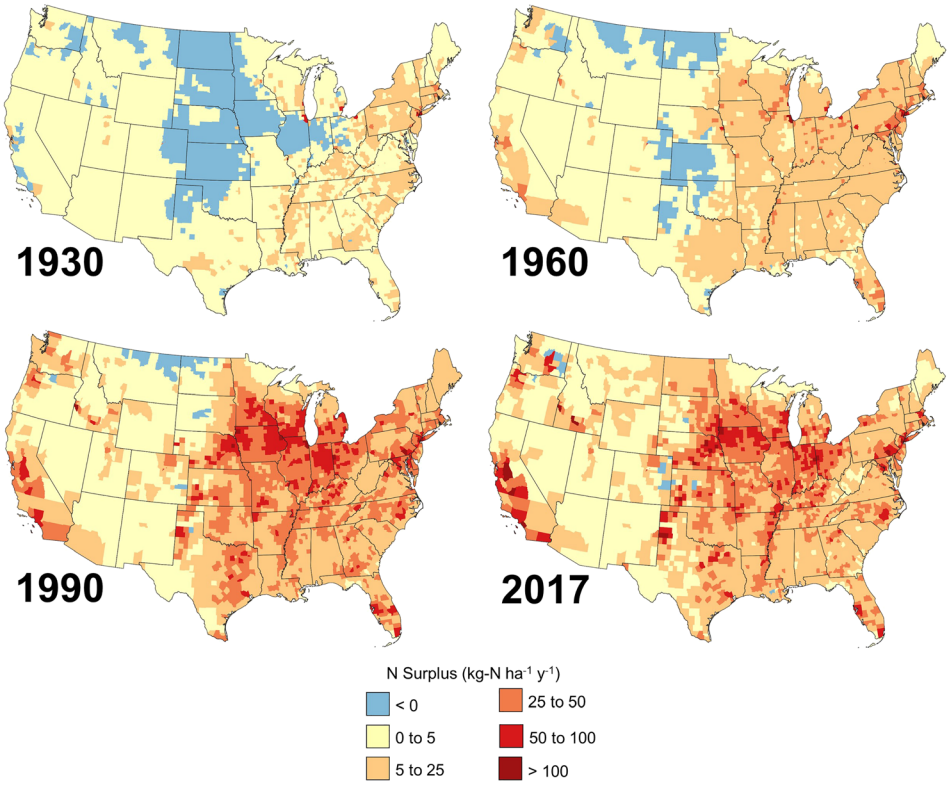

Figure 2. County-scale N surplus (NS_{cnty}, kg N ha^{-1} y^{-1}) maps for the contiguous United States for (a) 1930, (b), 1960, (c) 1990, and (d) 2017.

value being considered optimal (Kodinariya & Makwana, 2013). As noted by Kodinariya and Makwana (2013), the elbow cannot always be unambiguously identified. To address this, we supplemented the Elbow Method with a visual inspection of resulting clustered N trajectories to confirm whether including additional clusters provided additional insight into spatial and temporal variations in N dynamics.

2.2.2. N Surplus Clusters

For the cluster analysis of N surplus trajectories, we split the NS_{cnty} time series for individual counties into five time periods, the same as those used for analysis individual components (section 2.2.1). As with the component trajectories, we included the mean magnitude and the linear slope for NS_{cnty} for each period. In addition, we included the mean fractional contribution of each input component (*FERT*, *BNF*, *MAN*, *DEP*, *HUM*) to the total N input magnitude over the entire time period, thus providing a total of 15 features for the NS_{cnty} *k*-means analysis. Methods employed for the remainder of the analysis were identical to those used in the clustering of individual components.

3. Results and Discussion

3.1. County-Scale N Surplus Across the Contiguous United States

Our results show a sevenfold increase in the county-scale N surplus across the contiguous United States between 1930 and 2017, from a median value of 2.62 (IQR 0.47–4.69) kg N ha^{-1} y^{-1} in 1930 to 18.5 (IQR 8.82–33.4) kg N ha^{-1} y^{-1} in 2017, with specific areas emerging as hotspots over time (Figure 2). In the 1930s, the county-scale N surplus ranged from a median magnitude of 0.30 (IQR −3.52 to 1.60) kg N ha^{-1} y^{-1} in the Great Plains states to values greater than 200 kg N ha^{-1} y^{-1} in large urban areas such as San Francisco and New York City. An East-West gradient can be seen in NS_{cnty} magnitudes, with higher values in the Northeastern and Mid-Atlantic states driven by N in atmospheric deposition and livestock manure. Mineral N fertilizer use during this period was minimal.

By 1960, we see increases in the N surplus as a function of agricultural intensification, driven by post-WWII increases in the use of N fertilizer (Cao et al., 2018). Increases are particularly apparent in the midwestern Corn Belt. While in 1930, NS_{cnty} values in many midwestern counties were negative, indicative of agricultural production without sufficient replenishment of soil N, by 1960 the median NS_{cnty} magnitude was 8.8 (IQR 4.3–15.3) kg N ha^{-1} y^{-1} across the Corn Belt, and surplus values were in many counties more than 30 kg N ha^{-1} y^{-1} in agricultural areas of Illinois and Nebraska. By 1990, the Corn Belt truly emerged as the largest regional NS_{cnty} hot spot, with median magnitudes of 34.6 (IQR 18.0–47.3) kg N ha^{-1} y^{-1}. In 2017, Corn Belt states, as well as the California Central Valley continue as NS_{cnty} hot spots. In contrast, surplus values decreased in many nonurban Northeastern U.S. counties, driven by decreases in atmospheric N deposition (Lloret & Valiela, 2016).

3.2. Components of the N Balance

Cluster analysis was used to explore the dominant modes of behavior across the United States for the six components of the N mass balance: (a) human waste N, (b) atmospheric N deposition, (c) livestock manure N, (d) fertilizer N, (e) BNF, and (f) crop N uptake. The clustering was carried out based on temporal changes in N fluxes for individual components over time as well as the magnitudes of these county-scale fluxes. It is important to note that decisions regarding the number of clusters for each component and thus criteria for divisions between clusters are not absolute. The results do, however, allow us to better see key differences in temporal trajectories and to better identify spatially and temporally varying drivers of N dynamics, as described below.

3.2.1. Human Waste

Five clustered trajectories for human N waste were identified. These trajectories reflect the spatial distribution of human population across the United States as well as differences in the growth rates of various cities (Figure 3a). Cluster 5 and 6 counties contain a variety of medium to large U.S. cities (e.g., New York, Atlanta, Dallas–Fort Worth, Washington D.C., Chicago, and San Francisco). Cluster 6 counties have maintained high population densities, and thus high N inputs, across the entire time frame of analysis, with some migration out of the metropolitan areas evident after World War II due to suburbanization and increasing car ownership (Rieniets, 2009). Counties in Clusters 2, 3, and 4 are characterized by heterogeneous land use, often with high-density urban cores surrounded by lower density peri-urban areas or rural landscapes. Human waste N inputs in these areas have increased steadily, but moderately, over the study period, with a mean increase of 0.12 ± 0.13 kg N ha^{-1} y^{-1}. In contrast, human waste N inputs have remained flat in Cluster 1. Cluster 1 counties cover 90.8% of the country and are dominantly rural but contributed only 31.6% of the total human waste N inputs in 2017.

Regarding the relative importance of human waste N to overall N budgets across the United States, two major things should be noted. First, while N inputs in urban counties can in some cases greatly exceed those in agricultural counties due to the importance of N from human waste, the number of counties with these high inputs is very small. Counties in Clusters 5 and 6, for example, where human N waste inputs can be greater than 300 kg N ha^{-1} y^{-1}, make up only 0.2% of total area in the United States. Second, human waste in the United States is rarely discharged directly to the environment; it is estimated that 75% passes through a wastewater treatment plant, while the remaining 25% is treated via private septic systems (EPA, 2004, 2005). Therefore, despite the large N input magnitudes from human waste in densely populated urban areas, this input represents point source pollution that we have been successful in controlling, making it pose a much smaller risk to the aquatic environment.

3.2.2. Atmospheric N Deposition

U.S. trends in atmospheric N deposition show spatial and temporal patterns consistent with NO_x emissions as well as the implementation of Clean Air Act regulations, as demonstrated by the five identified clusters (Figure 3b). More than 80% of North American emissions of reactive N are anthropogenic, with most originating from fossil fuel combustion associated with motor vehicle use and power generation (Galloway et al., 2008; Howarth et al., 2002). Accordingly, there is a general east-west gradient in deposition rates, with the lower deposition clusters occurring in the Mountain West and the western Midwest Plains states (Clusters 1 and 2). These spatial dynamics can be attributed to the higher population densities and emission rates in the eastern United States as well as the prevalent west-to-east air mass transport trajectory across the continent (Butler et al., 2003; Lloret & Valiela, 2016). The highest rates of deposition (Cluster 5: a peak above

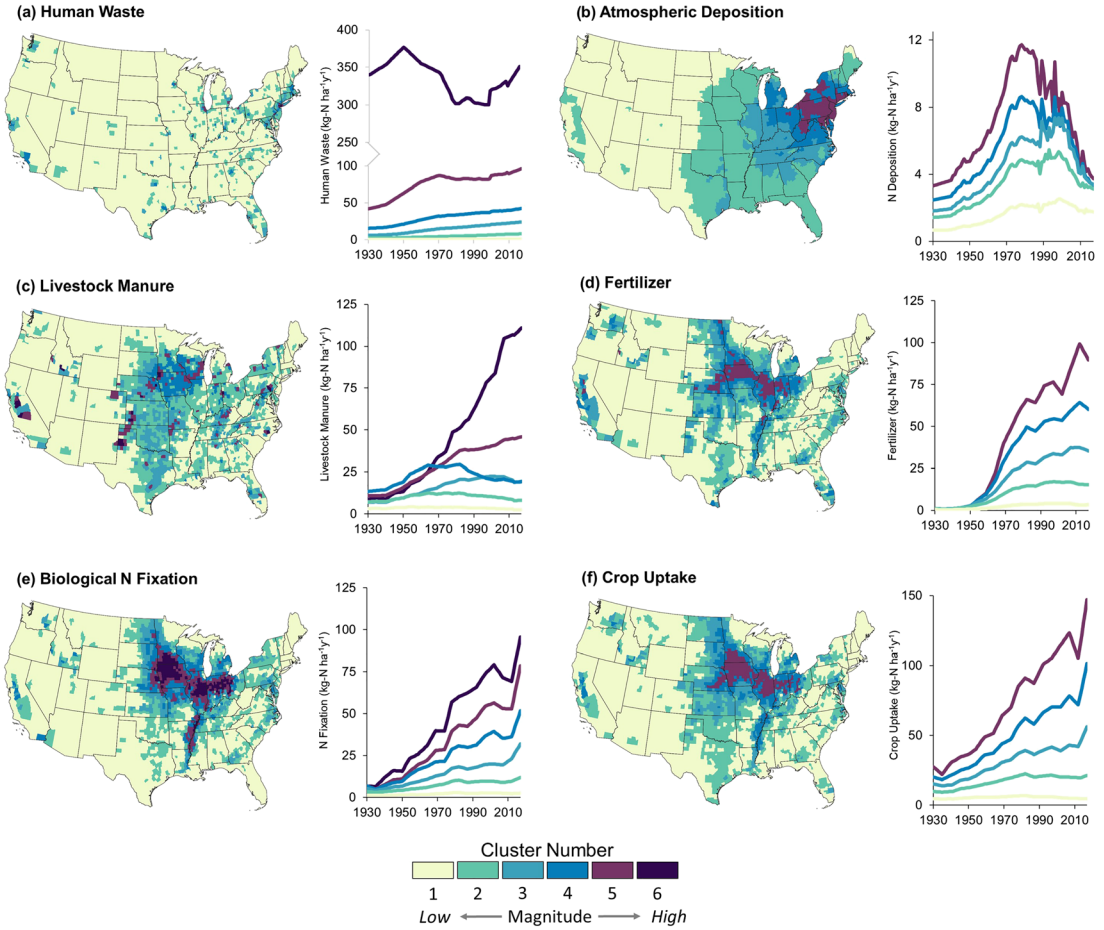

Figure 3. Cluster results for each component of the N mass balance: (a) Human waste N, (b) atmospheric N deposition, (c) livestock manure N, (d) N fertilizer, (e) biological N fixation, and (f) crop N uptake, all in kg N ha^{-1} y^{-1}. Each component is divided into either 5 or 6 individual clusters based on *k*-means clustering of magnitude and slope characteristics of the county-scale time trajectories. Each plotted trajectory represents a time series for one cluster, with the time series line corresponding to mean values for all counties included in that cluster. The counties belonging to each cluster are shown in the map with colors corresponding to those used in the time series plots. To see all county trajectories in each cluster, see Figure S1.

11.7 kg N ha^{-1} y^{-1} in 1978) occur in the northeastern states of New York, New Jersey, and Pennsylvania, where high deposition rates have severely impacted ecosystems, causing degradation of forested land, acidification of surface waters, and perturbation of the natural N cycle (Kahl et al., 2004; Lloret & Valiela, 2016). Temporally, atmospheric deposition across the United States has been decreasing for at least the last three decades, primarily due to progressively more stringent regulations related to NO_x emissions, including 1990 amendments to the Clean Air Act (Lloret & Valiela, 2016). The rate of decline is highest for the eastern states with the highest deposition rates and the lowest in the western states, where there is less industry, and deposition rates are lower.

3.2.3. Manure N

The spatiotemporal patterns of livestock N excretion provide evidence of a trend toward the centralization of U.S. livestock production (Figure 3c). Between 1930 and 1950, livestock production was more integrated across agricultural regions, and there was less variability in manure N inputs across counties (6.6 ± 4.5 kg N ha^{-1} y^{-1}; CV = 0.67). By 2017, however, the variability in manure N inputs across counties had doubled (10.0 ± 13.7 kg N ha^{-1} y^{-1}; CV = 1.37). This transition is especially apparent in Cluster 6 counties, which are areas of intensive livestock production scattered throughout the United States, including the Texas panhandle, the California Central Valley, and Pennsylvania's Lancaster County. Between 1930 and 1950, mean manure N inputs in Cluster 6 counties (10.5 ± 7.1 kg N ha^{-1} y^{-1}) were close to the national mean. After 1950, however, manure N production for these counties began to increase, and by 1965, the magnitudes surpassed those in all other counties. After 1965, Cluster 6 manure N production increased at

a rate of approximately 1.7 ± 0.6 kg N ha^{-1} y^{-1}. At the same time, production rates began to decrease in Cluster 2 and Cluster 4 counties. Though the rates of decrease are relatively small (−0.09 ± 0.12 and −0.23 ± 0.2 kg N ha^{-1} y^{-1}), this area of decrease constitutes approximately 25.6% of the contiguous United States. Such changes provide evidence of a transition from a more diversified agricultural landscape, where small farms and livestock operations coexisted across the country (Hilimire, 2011), to more concentrated animal operations, which characterize the current production system.

3.2.4. Fertilizer N

Fertilizer N is the second-largest input to the national-scale N budget after human waste, and its use in the United States has increased more than 20-fold since 1945. While fertilizer application rates began increasing across the entire country between 1945 and 1980, the rates of increase varied across the five identified clusters (Figure 3d). The largest increases occurred in Cluster 4 and Cluster 5 counties, which are primarily located in the Midwestern Corn Belt and California's Central Valley (Cluster 4, 1.4 ± 0.3 kg N ha^{-1} y^{-1}; Cluster 5, 2.0 ± 0.32 kg N ha^{-1} y^{-1}). For these two high-input clusters, the county-scale 2017 fertilizer N inputs were approximately 60.2 ± 9.9 and 89.7 ± 11.0 kg N ha^{-1} y^{-1}, respectively. While in the Corn Belt, fertilizer N application is primarily supporting corn and soybean production, in California's Central Valley, the high fertilizer inputs are supporting the production of more than half of U.S.-grown fruits, nuts, and vegetables (Keppen & Dutcher, 2015). Cluster 1 counties, which continue to maintain very low rates of fertilizer use (3.4 ± 3.0 kg N ha^{-1} y^{-1}), include grassland and shrubland areas of the Western United States, which have little agriculture (Waisanen & Bliss, 2002).

3.2.5. Biological N Fixation

While all leguminous plants fix N, BNF in U.S. agriculture is contingent upon the growth of two primary crops: soybeans and alfalfa hay. In the 1930s, alfalfa accounted for 35% of all agricultural BNF, but by 2017, its contribution had shrunk to only 15%. Soybean production, however, increased 500-fold during this period. Although soybeans had been introduced to the United States in the 18th century, they became important as a major commodity in the United States during the 1940s, when World War II increased the demand for oils, lubricants, and plastics, all of which could be met by domestic soybean production (Hymowitz & Shurtleff, 2005). Soybean production increased even more after the war, as soybeans were shipped overseas as part of U.S. foreign-aid programs, and livestock producers began using soybean meal as a primary protein source for poultry, hogs, and cattle (Houck et al., 1972). For the Cluster 5 and Cluster 6 counties, which have the highest 2017 rates of BNF, soybean N fixation increased from less than 5% of all BNF in 1930 to more than 95% of all BNF in 2017 (Figure 3e). In contrast, Cluster 1 counties, where BNF rates are the lowest, have exhibited relatively flat trends for BNF (0.01 ± 0.01 kg N ha^{-1} y^{-1}) between 1930 and 2017, and soybean N fixation still accounts for only approximately 13.2% of all crop BNF.

3.2.6. Crop N Uptake

Crop uptake is the only N output pathway in our mass balance, and the spatiotemporal patterns of uptake are closely correlated with patterns for fertilizer N application and BNF (Figure 3f). We identified five primary clusters for crop N uptake trajectories. Clusters 4 and 5 have the largest 2017 uptake magnitudes (Cluster 4, 101 ± 20.9 kg N ha^{-1} y^{-1}; Cluster 5, 147 ± 18.5 kg N ha^{-1} y^{-1}) and account for 22.5% and 24.8% of uptake at the U.S. scale, despite occupying only 3.6% and 5.8% of the overall area, respectively. While crop N uptake has plateaued in Clusters 1 and 2, Clusters 4 and 5 continue to exhibit increases in crop production and therefore increases in N uptake. Cluster 1 counties, where mean uptake rates have remained low (4.7 ± 4.0 kg N ha^{-1} y^{-1}, 2017), represent areas of the United States where there is little row-crop agriculture, with harvested areas currently constituting less than 5% of total land area.

3.3. N Surplus Trajectories Across the Contiguous United States

We examined county-scale N surplus trajectories for the more than 3,000 counties across the contiguous United States and, based on the clustering algorithm described in section 2.2.2, identified 10 distinct N trajectories (Figures 4 and 5). These include three crop-dominated clusters (C1, C2, and C3), four livestock-dominated clusters (L1, L2, L3, and L4), two urban-dominated clusters (U1 and U2), and one cluster for minimally impacted landscapes (M1). For the three crop-dominated clusters, fertilizer is the primary N input (Figures 4a and 5a). Of these, C1 has substantially greater N surplus magnitudes than the other two. N surplus magnitudes began increasing in the C1 cluster counties in approximately 1950, concurrent with increases in fertilizer application. Magnitudes continued to increase until 1980, after which they plateaued at approximately 40–50 kg N ha^{-1} y^{-1} (Figure 4a). Plateau values were reached in the C2 and C3 counties

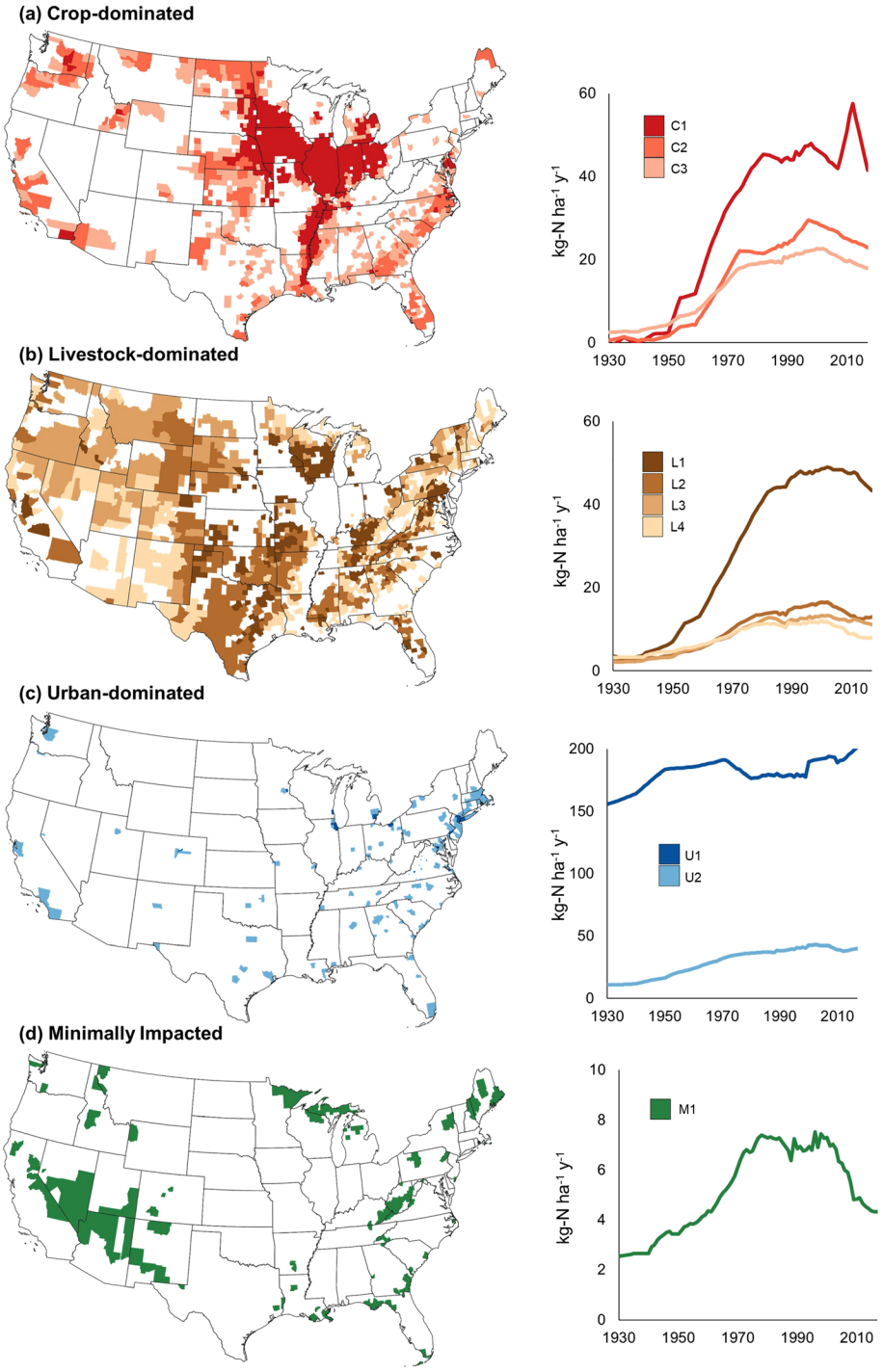

Figure 4. N surplus clusters across the contiguous United States. We have identified 10 primary clustered trajectories, with the clusters being differentiated as a function of the slopes of the N surplus trajectories, the N surplus magnitudes, and the dominant input component. Time trajectories of the clusters for (a) crop production, (b) livestock production, (c) human waste flows, and (d) atmospheric deposition. To see all trajectories on a single axis, see Figure S2.

earlier in the 1970s, remaining close to 20 kg N ha^{-1} y^{-1}. While all three cropland clusters appear to have plateaued, a spike in the N surplus can be seen for the C1 cluster in 2012. This spike can be attributed to 2012 being a drought year, which led to high rates of crop failure (Mallya et al., 2013) and thus low crop N uptake and a large N surplus. The four livestock-dominated clusters also demonstrate N surplus plateau

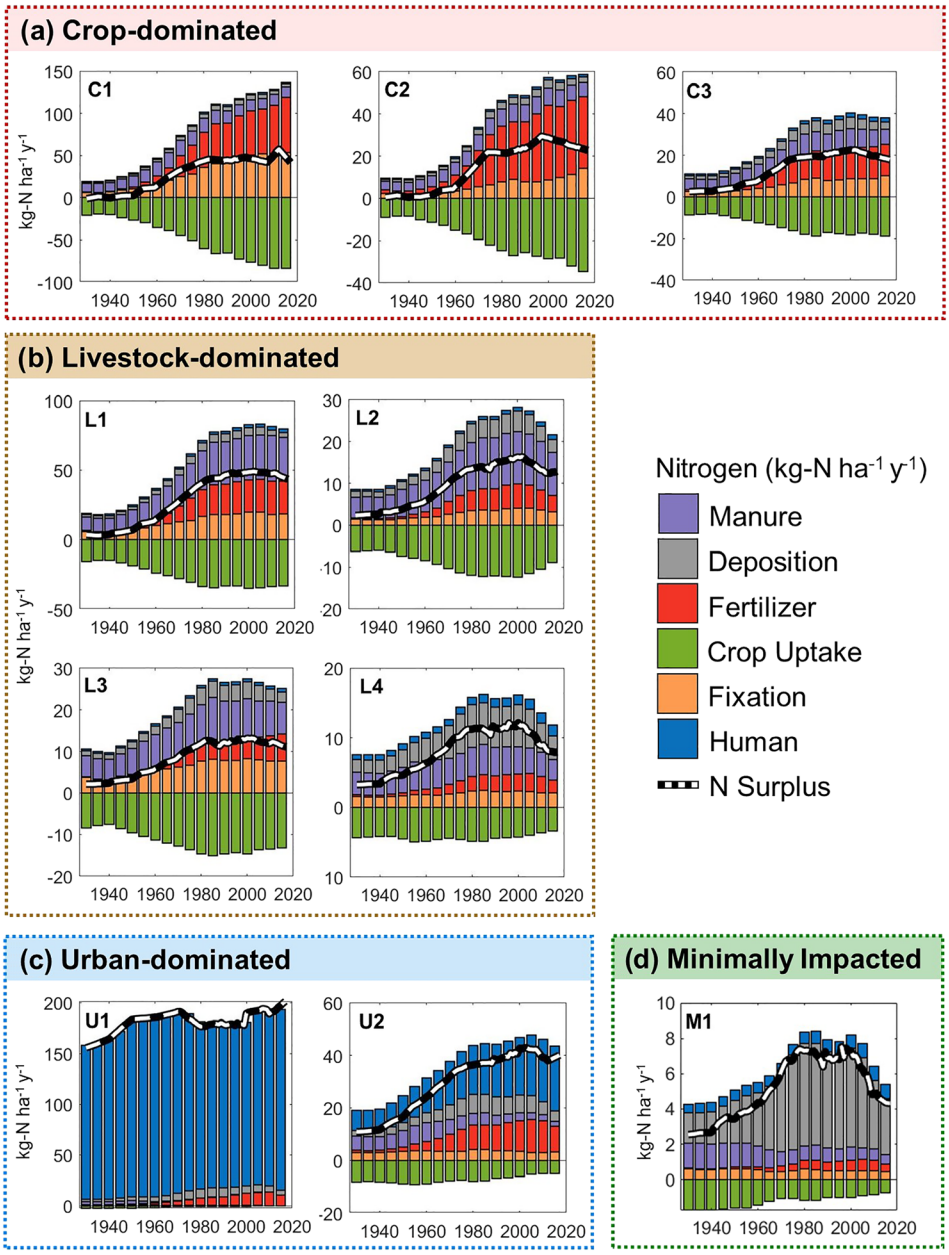

Figure 5. Components of the N mass balance over time for the 10 N surplus clusters. Mean county-scale magnitudes for individual components of the N mass balance are shown, with inputs (manure, atmospheric deposition, fertilizer, biological N fixation, and human waste) and outputs (crop uptake) shown as stacked bars. The time series are aggregated into four N surplus typologies: (a) crop-dominated; (b) livestock-dominated; (c) urban-dominated; and (d) minimally impacted.

behavior beginning in the 1970s to early 1980s, with the L1 cluster plateauing at magnitudes 2–3 times greater than those in the L2–L4 clusters (Figure 4b). The L1 clusters represent counties with large, concentrated animal operations, with manure N being the dominant N input (Figures 4b and 5b). Wisconsin, in particular, with its large dairy industry, is dominated by L1 counties. Kentucky, the Texas panhandle, and the California panhandle are other L1 hotspots. The N surplus trajectories for the two urban-dominated clusters show slowly increasing surplus values, tracking with increases in human population (Figures 4c and 5c). The magnitudes of N inputs for large urban areas (cluster U1) are the highest among all trajectories, increasing from 156 kg N ha^{-1} y^{-1} in 1930 to 201 kg N ha^{-1} y^{-1} in 2017. However, note that these values primarily represent human waste that is treated by wastewater treatment

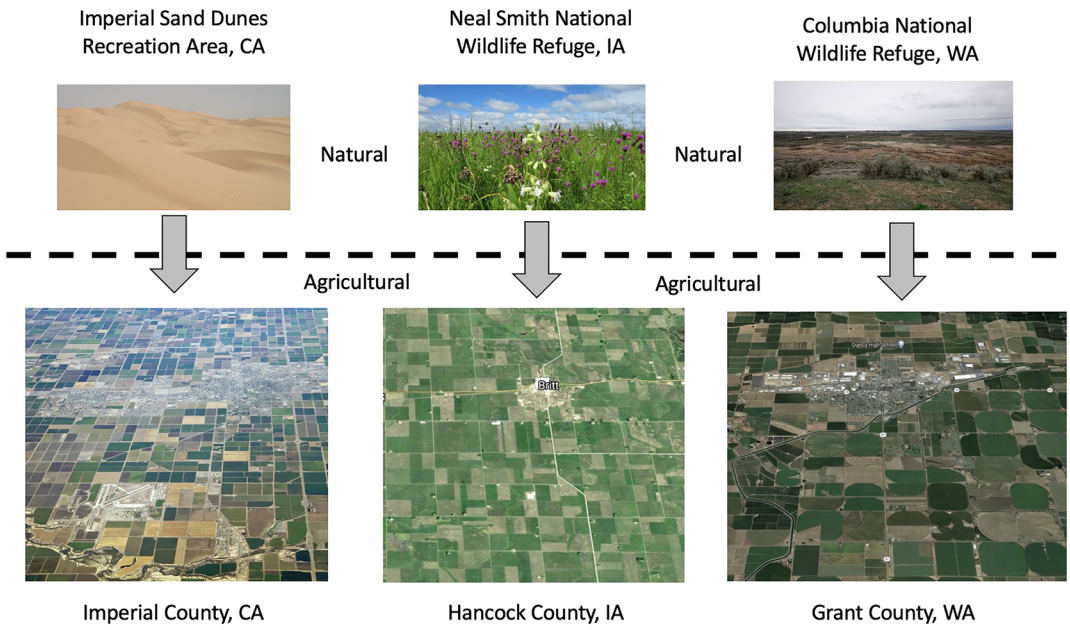

Figure 6. Conversion of climatically and geographically diverse natural landscape to homogenized agroecosystems. Nitrogen dynamics in these three counties are similarly dominated by crop production, despite large differences in temperatures and both the timing and magnitude of annual precipitation. Elimination of resource constraints, specifically access to irrigation water and application of commercial fertilizers, allows for homogenization of diverse rural landscapes. Similar results have been observed by Groffman et al. (2014) in urban landscapes.

plants before being discharged to aquatic systems, as noted in section 3.2.1. The "minimally impacted" cluster includes counties with very little agricultural land use and low population densities. In these counties, N surplus is dominated by atmospheric deposition, and thus the trajectories primarily follow trends in atmospheric N deposition (Figures 4d and 5d).

3.4. N Surplus and Landscape Homogenization

Interestingly, our results suggest that while the various N surplus clusters are, in the mean, associated with specific regions of the country, this association is not absolute. For example, as described in section 3.3, we identified three "crop-dominated" N Surplus clusters (C1–C3). In these counties, fertilizer N is a primary driver of the N mass balance. In Figure 5, we see that the C1 counties, which have the highest N surplus magnitudes, dominate in Iowa and other areas of the Corn Belt, a region responsible for 36% of global corn production (Green et al., 2018). The Corn Belt, on average, has 120 frost-free days, and mean annual precipitation is approximately 940 mm (Ort & Long, 2014). However, C1 counties can also be found in other areas that are climatically quite different (Figure 6). For example, southern California's Imperial County is located in a desert region that rarely experiences snow and where annual rainfall is less than 80 mm. Facilitated by irrigation water from the Colorado River, however, crop production in Imperial County dominates the county N budget, and the county follows the C1, crop-dominated N surplus trajectory (Collins, 2004). The crop-dominated C1 N dynamics of Grant County in central Washington are similarly facilitated by irrigation water from the Columbia River, pumped via power supplied by the Grand Coulee Dam (Ortolano & Cushing, 2000). Mean annual precipitation in Grant County is only 177 mm, and 70% of that precipitation falls during the winter months (Miller, 1948). With irrigation, however, Grant County is the leading agricultural county in Washington state based on crop sales and the 11th most important nationally (Granastein, 2014).

The similarities in N surplus trajectories across climatically diverse regions identified in the present study are indicative of a widespread functional homogenization of human-dominated landscapes. Such homogenization has been noted in both urban and rural landscapes. Urban lawns, for example, have been found to show more similarity to other lawns in geographically and climatically diverse cities than to adjacent native ecosystems (Groffman et al., 2014). Surface water features in urban areas have also been found to be more

similar to each other than to those in surrounding undeveloped landscapes (Steele & Heffernan, 2014). Indeed, it has been conjectured that urbanization may be one of the most homogenizing of human activities, as cities exist for centuries in a state of "disequilibrium" with the natural environment through the importation of large quantities of food, energy, and other materials (McKinney, 2006). At the same time, the urban demand for imports of food and energy drives a similar homogenization of agroecosystems. In rural areas, this homogenization may occur via the elimination of key resource constraints. For example, in the cases of Imperial County, CA, and Grant County, WA, we see access to irrigation water loosening resource limitations, allowing for the conversion of arid, fallow landscapes to intensive agriculture. Conversely, in Hancock County, IA, installation of tile drainage has allowed for conversion of wet prairie land to highly productive cropland (Basu et al., 2010; Boland-Brien et al., 2014; Van Meter & Basu, 2015). Nutrients are also required for plant growth, and widespread application of commercial fertilizers in crop-dominated regions eliminates deficits that would occur if the only source of nutrients was those occurring in native soils. Accordingly, fast increases in fertilizer N application rates in crop-dominated counties during the mid-20th century, and sustained N surplus magnitudes of approximately 40 kg N ha^{-1} y^{-1} are not just a simple reflection of agricultural homogenization but also a driver of that homogenization.

4. Conclusions

We have developed the TREND-nitrogen data set, which, for the first time, provides a comprehensive, 88-year (1930–2017) data set of county-scale N inputs (fertilizer, manure, biological N fixation, human waste, and atmospheric deposition) and nonhydrologic outputs (crop uptake) across the contiguous United States. Further, we have used machine-learning approaches to identify dominant patterns in N trajectories, both for individual components of the N mass balance and the net N surplus. The results of the cluster analysis allow us to understand long-term N dynamics and the ways in which patterns of N use have shaped diverse regions, resulting in a homogenization of rural landscapes.

This compilation of N data from disparate sources and across over 80 years represents an unprecedented opportunity for understanding spatiotemporal characteristics of anthropogenic N use and will be critical to advancing our understanding of the ways in which excess N impact water quality, GHG emissions, and ecosystem health across diverse landscapes. While county-scale N mass balance data for the United States has previously been available, these earlier data sets, due to limited digital availability of source data, have generally been limited to years since 1987. This new, longer time series will explicitly facilitate the modeling of long-term N dynamics across periods with significant changes in land use and management and will allow for explicit consideration of the impacts of legacy N—N that has accumulated over decades of intensive crop and livestock production—on environmental outcomes.

Data Availability Statement

The TREND-nitrogen data set used in this research is available at https://doi.org/10.1594/PANGAEA.917583.

Acknowledgments

We thank Linea Miller, Megan Jordan, Kathryn Starratt, Nicole Khun, Sara Dechant, and Caitlyn Watt for assistance with the data compilation. The authors have no competing interests to declare. The present work was financially supported by an NSERC Discovery Grant and by an Ontario Early Researcher Award, both awarded to N. B. B. and by startup funds for K. J. V. from the University of Illinois at Chicago. D. K. B was partially funded by the Queen Elizabeth II Graduate Scholarship in Science and Technology (QEII-GSST).

References

Alexander, P., Rounsevell, M. D. A., Dislich, C., Dodson, J. R., Engström, K., & Moran, D. (2015). Drivers for global agricultural land use change: The nexus of diet, population, yield and bioenergy. *Global Environmental Change: Human and Policy Dimensions*, *35*, 138–147. https://doi.org/10.1016/j.gloenvcha.2015.08.011

Alexander, R. B., & Smith, R. A. (1990). *County-level estimates of nitrogen and phosphorus fertilizer use in the United States, 1945 to 1985* (U.S. Geological Survey Open-File Report 90-130). Reston, VA: U.S. Geological Survey. https://doi.org/10.3133/ofr90130

Alexander, R. B., Smith, R. A., Schwartz, G. E., Preston, S. D., Brakebill, J. W., Srinivasan, R., & Pacheco, P. A. (2001). Atmospheric nitrogen flux from the watersheds of major estuaries of the United States: An application of the SPARROW watershed model. In R. A. Valigura, R. B. Alexander, M. S. Castro, T. P. Meyers, H. W. Paerl, P. E. Stacey, & R. E. Turner, (Eds.), *Nitrogen loading in coastal water bodies: An atmospheric perspective*, *Coastal and Estuarine Studies* (Vol. 57, pp. 119–170). Washington, DC: American Geophysical Union.

Ascott, M. J., Gooddy, D. C., Wang, L., Stuart, M. E., Lewis, M. A., Ward, R. S., & Binley, A. M. (2017). Global patterns of nitrate storage in the vadose zone. *Nature Communications*, *8*, 1416. https://doi.org/10.1038/s41467-017-01321-w

Ay, M., & Kisi, O. (2014). Modelling of chemical oxygen demand by using ANNs, ANFIS and *k*-means clustering techniques. *Journal of Hydrology*, *511*, 279–289. https://doi.org/10.1016/j.jhydrol.2014.01.054

Basu, N. B., Destouni, G., Jawitz, J. W., Thompson, S. E., Loukinova, N. V., Darracq, A., et al. (2010). Nutrient loads exported from managed catchments reveal emergent biogeochemical stationarity. *Geophysical Research Letters*, *37*, L23404. https://doi.org/10.1029/2010gl045168

Boland-Brien, S. J., Basu, N. B., & Schilling, K. E. (2014). Homogenization of spatial patterns of hydrologic response in artificially drained agricultural catchments. *Hydrological Processes*, *28*(19), 5010–5020. https://doi.org/10.1002/hyp.9967

Bouwman, A. F., Van Drescht, G., & Van der Hoek, K. W. (2005). Global and regional surface nitrogen balances in intensive agricultural production systems for the period 1970-2030. *Pedosphere*, *15*(2), 135–155.

Boyer, E. W., Goodale, C. L., Jaworski, N. A., & Howarth, R. W. (2002). Anthropogenic nitrogen sources and relationships to riverine nitrogen export in the northeastern USA. *Biogeochemistry*, *57*, 137–169. https://doi.org/10.1023/A:1015709302073

Brakebill, J. W., & Gronberg, J. M. (2017). *County-level estimates of nitrogen and phosphorus from commercial fertilizer for the conterminous United States, 1987-2012*. Reston, VA: U.S. Geological Survey. https://doi.org/10.5066/F7H41PKX

Butler, T. J., Likens, G. E., Vermeylen, F. M., & Stunder, B. J. B. (2003). The relation between NO_x emissions and precipitation NO_{3-} in the eastern USA. *Atmospheric Environment*, *37*(15), 2093–2104. https://doi.org/10.1016/S1352-2310(03)00103-1

Byrnes, D. K., Van Meter, K. J., & Basu, N. B. (2020). *Trajectories Nutrient Dataset for Nitrogen (TREND-nitrogen)*. PANGAEA.

Camargo, J. A., & Alonso, A. (2006). Ecological and toxicological effects of inorganic nitrogen pollution in aquatic ecosystems: A global assessment. *Environment International*, *32*(6), 831–849. https://doi.org/10.1016/j.envint.2006.05.002

Cao, P., Lu, C., & Yu, Z. (2018). Historical nitrogen fertilizer use in agricultural ecosystems of the contiguous United States during 1850–2015: Application rate, timing, and fertilizer types. *Earth System Science Data*, *10*(2), 969–984. https://doi.org/10.5194/essd-10-969-2018

Chen, D., Huang, H., Hu, M., & Dahlgren, R. A. (2014). Influence of lag effect, soil release, and climate change on watershed anthropogenic nitrogen inputs and riverine export dynamics. *Environmental Science & Technology*, *48*(10), 5683–5690. https://doi.org/10.1021/es500127t

Collins, K. (2004). *Imperial-Mexicali Valleys: Development and environment of the U.S.-Mexican border region*. SCERP and IRSC publications.

Del Grosso, S., Ojima, D., Parton, W., Mosier, A., Peterson, G., & Schimel, D. (2002). Simulated effects of dryland cropping intensification on soil organic matter and greenhouse gas exchanges using the DAYCENT ecosystem model. *Environmental Pollution*, *116*, S75–S83. https://doi.org/10.1016/S0269-7491(01)00260-3

Dentener, F. J. (2006). Global maps of atmospheric nitrogen deposition, 1860, 1993, and 2050. ORNL Distributed Active Archive Center. https://doi.org/10.3334/ORNLDAAC/830

Donner, S. D., Kucharik, C. J., & Foley, J. A. (2004). Impact of changing land use practices on nitrate export by the Mississippi River. *Global Biogeochemical Cycles*, *18*, GB1028. https://doi.org/10.1029/2003gb002093

Dubrovsky, N. M., Burow, K. R., Clark, G. M., Gronberg, J. A. M., Hamilton, P. A., Hitt, K. J., et al. (2010). *Nutrients in the nation's streams and groundwater, 1992–2004, Circular 1350*. Reston, VA: U.S. Geological Survey.

EPA. (2004). Primer for municipal wastewater treatment systems (No. 832-R-04-001). U.S. Environmental Protection Agency.

EPA. (2005). Handbook for managing onsite and clustered (Decentralized) wastewater treatment systems: An introduction to management tools and information for implementing EPA's management guidelines (No. 821-B-05-001). Environmental Protection Agency.

Galloway, J. N., Schlesinger, W. H., Hiram, L., Schnoor, L., & Tg, N. (1995). Nitrogen fixation: Anthropogenic enhancement-environmental response reactive N. *Global Biogeochemical Cycles*, *9*(2), 235–252. https://doi.org/10.1029/95GB00158

Galloway, J. N., Townsend, A. R., Erisman, J. W., Bekunda, M., Cai, Z., Freney, J. R., et al. (2008). Transformation of the nitrogen cycle: Recent trends, questions, and potential solutions. *Science*, *320*(5878), 889–892. https://doi.org/10.1126/science.1136674

Goyette, J.-O., Bennett, E. M., Howarth, R. W., & Maranger, R. (2016). Changes in anthropogenic nitrogen and phosphorus inputs to the St. Lawrence sub-basin over 110 years and impacts on riverine export. *Global Biogeochemical Cycles*, *30*, 1000–1014. https://doi.org/10.1002/2016GB005384

Granastein, D. (2014, May 28). Washington Agriculture by the Numbers | CSANR | Washington State University. Retrieved February 7, 2020, from http://csanr.wsu.edu/wa-ag-by-the-numbers/

Green, T. R., Kipka, H., David, O., & McMaster, G. S. (2018). Where is the USA Corn Belt, and how is it changing? *The Science of the Total Environment*, *618*, 1613–1618. https://doi.org/10.1016/j.scitotenv.2017.09.325

Grizzetti, B., Bouraoui, F., de Marsily, G., & Bidoglio, G. (2005). A statistical approach to estimate nitrogen sectorial contribution to total load. *Water Science and Technology: A Journal of the International Association on Water Pollution Research*, *51*(3–4), 83–90. https://doi.org/10.2166/wst.2005.0578

Groffman, P. M., Cavender-Bares, J., Bettez, N. D., Grove, J. M., Hall, S. J., Heffernan, J. B., et al. (2014). Ecological homogenization of urban USA. *Frontiers in Ecology and the Environment*, *12*, 74–81. https://doi.org/10.1890/120374

Gu, B., Ge, Y., Chang, S. X., Luo, W., & Chang, J. (2013). Nitrate in groundwater of China: Sources and driving forces. *Global Environmental Change: Human and Policy Dimensions*, *23*(5), 1112–1121. https://doi.org/10.1016/j.gloenvcha.2013.05.004

Haines, M., Fishback, P., & Rhode, P. (2018). United States Agriculture Data, 1840–2012 [Data set]. https://doi.org/10.3886/ICPSR35206.v4

Hamlin, Q. F., Kendall, A. D., Martin, S. L., Whitenack, H. D., Roush, J. A., Hannah, B. A., & Hyndman, D. W. (2020). Quantifying landscape nutrient inputs with spatially explicit nutrient source estimate maps. *Journal of Geophysical Research: Biogeosciences*, *125*, e2019JG005134. https://doi.org/10.1029/2019jg005134

Han, H., & Allan, J. D. (2008). Estimation of nitrogen inputs to catchments: Comparison of methods and consequences for riverine export prediction. *Biogeochemistry*, *91*(2–3), 177–199. https://doi.org/10.1007/s10533-008-9279-3

Hansen, B., Thorling, L., Schullehner, J., Termansen, M., & Dalgaard, T. (2017). Groundwater nitrate response to sustainable nitrogen management. *Scientific Reports*, *7*, 8566. https://doi.org/10.1038/s41598-017-07147-2

Harding, L. W. Jr., Mallonee, M. E., Perry, E. S., Miller, W. D., Adolf, J. E., Gallegos, C. L., & Paerl, H. W. (2019). Long-term trends, current status, and transitions of water quality in Chesapeake Bay. *Scientific Reports*, *9*, 6709. https://doi.org/10.1038/s41598-019-43036-6

Hartigan, J. A., & Wong, M. A. (1979). Algorithm AS 136: A *k*-means clustering algorithm. *Journal of the Royal Statistical Society. Series C, Applied Statistics*, *28*(1), 100–108. https://doi.org/10.2307/2346830

Hilimire, K. (2011). Integrated crop/livestock agriculture in the United States: A review. *Journal of Sustainable Agriculture*, *35*(4), 376–393. https://doi.org/10.1080/10440046.2011.562042

Hong, B., Swaney, D. P., & Howarth, R. W. (2011). A toolbox for calculating net anthropogenic nitrogen inputs (NANI). *Environmental Modelling and Software*, *26*(5), 623–633. https://doi.org/10.1016/j.envsoft.2010.11.012

Hong, B., Swaney, D. P., & Howarth, R. W. (2013). Estimating net anthropogenic nitrogen inputs to U.S. watersheds: Comparison of methodologies. *Environmental Science and Technology*, *47*(10), 5199–5207. https://doi.org/10.1021/es303437c

Hong, B., Swaney, D. P., Mörth, C. M., Smedberg, E., Eriksson Hägg, H., Humborg, C., et al. (2012). Evaluating regional variation of net anthropogenic nitrogen and phosphorus inputs (NANI/NAPI), major drivers, nutrient retention pattern and management implications in the multinational areas of Baltic Sea basin. *Ecological Modelling*, *227*, 117–135. https://doi.org/10.1016/j.ecolmodel.2011.12.002

Houck, J. P., Ryan, M. E., & Subotnik, A. (1972). *Soybeans and their products: Markets, models, and policy*. Minneapolis, MN: University of Minnesota Press.

Houlton, B. Z., Boyer, E., Finzi, A., Galloway, J., Leach, A., Liptzin, D., et al. (2013). Intentional versus unintentional nitrogen use in the United States: Trends, efficiency and implications. *Biogeochemistry*, *114*, 11–23. https://doi.org/10.1007/s10533-012-9801-5

Howarth, R. W., Boyer, E. W., Pabich, W. J., & Galloway, J. N. (2002). Nitrogen use in the United States from 1961–2000 and potential future trends. *Ambio: A Journal of the Human Environment*, *31*(2), 88–96. https://doi.org/10.1579/0044-7447-31.2.88

Howarth, R. W., Swaney, D. P., Boyer, E. W., Marino, R., Jaworski, N., & Goodale, C. (2006). The influence of climate on average nitrogen export from large watersheds in the Northeastern United States. *Biogeochemistry*, *79*(1–2), 163–186. https://doi.org/10.1007/s10533-006-9010-1

Hudiburg, T. W., Wang, W., Khanna, M., Long, S. P., Dwivedi, P., Parton, W. J., et al. (2016). Impacts of a 32-billion-gallon bioenergy landscape on land and fossil fuel use in the US. *Nature Energy*, *1*, 15005. https://doi.org/10.1038/nenergy.2015.5

Hymowitz, T., & Shurtleff, W. R. (2005). Debunking soybean myths and legends in the historical and popular literature. *Crop Science*, *45*(2), 473–476. https://doi.org/10.2135/cropsci2005.0473

Ilampooranan, I., Van Meter, K. J., & Basu, N. B. (2019). A race against time: Modelling time lags in watershed response. *Water Resources Research*, *55*, 3941–3959. https://doi.org/10.1029/2018WR023815

Kahl, J. S., Stoddard, J. L., Haeuber, R., Paulsen, S. G., Birnbaum, R., Deviney, F. A., et al. (2004). Have U.S. surface waters responded to the 1990 Clean Air Act amendments? *Environmental Science & Technology*, *38*(24), 484A–490A. https://doi.org/10.1021/es040686l

Keppen, D., & Dutcher, T. (2015). The 2014 drought and water management policy impacts on California's Central Valley food production. *Journal of Environmental Studies and Sciences*, *5*, 362–377. https://doi.org/10.1007/s13412-015-0283-3

Kodinariya, T. M., & Makwana, P. R. (2013). Review on determining number of cluster in *k*-means clustering. *Aquatic Microbial Ecology: International Journal*, *1*, 90–95.

Kopáček, J., Hejzlar, J., & Posch, M. (2013). Factors controlling the export of nitrogen from agricultural land in a large central European catchment during 1900-2010. *Environmental Science & Technology*, *47*, 6400–6407. https://doi.org/10.1021/es400181m

Lassaletta, L., Billen, G., Grizzetti, B., Anglade, J., & Garnier, J. (2014). 50 year trends in nitrogen use efficiency of world cropping systems: The relationship between yield and nitrogen input to cropland. *Environmental Research Letters: ERL [Web Site]*, *9*, 105011. https://doi.org/10.1088/1748-9326/9/10/105011

Likas, A., Vlassis, N., & Verbeek, J. J. (2003). The global *k*-means clustering algorithm. *Pattern Recognition*, *36*(2), 451–461. https://doi.org/10.1016/S0031-3203(02)00060-2

Lloret, J., & Valiela, I. (2016). Unprecedented decrease in deposition of nitrogen oxides over North America: The relative effects of emission controls and prevailing air-mass trajectories. *Biogeochemistry*, *129*, 165–180. https://doi.org/10.1007/s10533-016-0225-5

MacKay, D. J. C. (2003). *Information theory, Inference and learning algorithms*. Cambridge, UK: Cambridge University Press.

Mallya, G., Zhao, L., Song, X. C., Niyogi, D., & Govindaraju, R. S. (2013). 2012 Midwest drought in the United States. *Journal of Hydrologic Engineering*, *18*, 737–745. https://doi.org/10.1061/(ASCE)HE.1943-5584.0000786

Mayorga, E., Seitzinger, S. P., Harrison, J. A., Dumont, E., Beusen, A. H. W., Bouwman, A. F., et al. (2010). Global nutrient export from WaterSheds 2 (NEWS 2): Model development and implementation. *Environmental Modelling & Software*, *25*(7), 837–853. https://doi.org/10.1016/j.envsoft.2010.01.007

McKinney, M. L. (2006). Urbanization as a major cause of biotic homogenization. *Biological Conservation*, *127*(3), 247–260. https://doi.org/10.1016/j.biocon.2005.09.005

Metson, G. S., MacDonald, G. K., Haberman, D., Nesme, T., & Bennett, E. M. (2016). Feeding the Corn Belt: Opportunities for phosphorus recycling in U.S. agriculture. *The Science of the Total Environment*, *542*, 1117–1126. https://doi.org/10.1016/j.scitotenv.2015.08.047

Miller, E. E. (1948). Geography of Grant County, Washington. *Economic Geography*, *24*(1), 19–27. https://doi.org/10.2307/141035

Mosier, A. R., Syers, J. K., & Freney, J. R. (2004). Nitrogen fertilizer: An essential component of increased food, feed, and fiber production. *Agriculture and the Nitrogen Cycle: Assessing the Impacts of Fertilizer Use on Food Production and the Environment*, *65*, 3–15.

National Atmospheric Deposition Program. (2018). NADP total deposition maps. Retrieved February 1, 2019, from http://nadp.slh.wisc.edu/committees/tdep/tdepmaps/

Ort, D. R., & Long, S. P. (2014, May 2). Limits on yields in the Corn Belt. *Science*, *344*, 484–485. https://doi.org/10.1126/science.1253884

Ortolano, L., & Cushing, K. K. (2000). Grand Coulee Dam and the Columbia Basin Project USA. World Commission on Dams. Retrieved from http://dina.centre-cired.fr/IMG/pdf/F9_GranCouleeDam.pdf

Rabalais, N. N., Turner, R. E., Dortch, Q., Justic, D., Bierman, V. J., & Wiseman, W. J. (2002). Nutrient-enhanced productivity in the northern Gulf of Mexico: Past, present and future. In E. Orive, M. Elliott, & V. N. de Jonge (Eds.), *Nutrients and Eutrophication in Estuaries and Coastal Waters: Proceedings of the 31st Symposium of the Estuarine and Coastal Sciences Association (ECSA), held in Bilbao, Spain, 3–7 July 2000* (pp. 39–63). Dordrecht: Springer Netherlands.

Rieniets, T. (2009). Shrinking cities: Causes and effects of urban population losses in the twentieth century. *Nature and Culture*, *4*(3), 231–254. https://doi.org/10.3167/nc.2009.040302

Rockström, J., Steffen, W., Noone, K., Persson, Å., Chapin, F. S. I. I. I., Lambin, E., et al. (2009). Planetary boundaries: Exploring the safe operating space for humanity. *Ecology and Society*, *14*, 32. Retrieved from https://pdxscholar.library.pdx.edu/iss_pub/64/. https://doi.org/10.5751/ES-03180-140232

Sabo, R. D., Clark, C. M., Bash, J., Sobota, D., Cooter, E., Dobrowolski, J. P., et al. (2019). Decadal shift in nitrogen inputs and fluxes across the contiguous United States: 2002–2012. *Journal of Geophysical Research: Biogeosciences*, *124*, 3104–3124. https://doi.org/10.1029/2019JG005110

Schullehner, J., Hansen, B., Thygesen, M., Pedersen, C. B., & Sigsgaard, T. (2018). Nitrate in drinking water and colorectal cancer risk: A nationwide population-based cohort study. *International Journal of Cancer*, *143*(1), 73–79. https://doi.org/10.1002/ijc.31306

Sebilo, M., Mayer, B., Nicolardot, B., Pinay, G., & Mariotti, A. (2013). Long-term fate of nitrate fertilizer in agricultural soils. *Proceedings of the National Academy of Sciences*, *110*, 18,185–18,189. https://doi.org/10.1073/pnas.1305372110

Smil, V. (1999). Detonator of the population explosion. *Nature*, *400*(6743), 415–415. https://doi.org/10.1038/22672

Steele, M. K., & Heffernan, J. B. (2014). Morphological characteristics of urban water bodies: Mechanisms of change and implications for ecosystem function. *Ecological Applications: A Publication of the Ecological Society of America*, *24*(5), 1070–1084. https://doi.org/10.1890/13-0983.1

Swaney, D. P., Hong, B., Ti, C., Howarth, R. W., & Humborg, C. (2012). Net anthropogenic nitrogen inputs to watersheds and riverine N export to coastal waters: A brief overview. *Current Opinion in Environmental Sustainability*, *4*(2), 203–211. https://doi.org/10.1016/j.cosust.2012.03.004

Swaney, D. P., & Howarth, R. W. (2019). County, subregional and regional phosphorus data derived from the net anthropogenic nitrogen/phosphorus inputs (NANI/NAPI) toolbox. *Data in Brief*, *25*, 104265. https://doi.org/10.1016/j.dib.2019.104265

Swaney, D. P., Howarth, R. W., & Hong, B. (2018). Nitrogen use efficiency and crop production: Patterns of regional variation in the United States, 1987–2012. *The Science of the Total Environment*, *635*, 498–511. https://doi.org/10.1016/j.scitotenv.2018.04.027

Syakila, A., & Kroeze, C. (2011). The global nitrous oxide budget revisited. *Greenhouse Gas Measurement and Management*, *1*(1), 17–26. https://doi.org/10.3763/ghgmm.2010.0007

U.S. Census Bureau. (2007). Census U.S. Decennial County population data, 1900-1990. Retrieved from http://www.nber.org/data/census-decennial-population.html

U.S. Census Bureau. (2016). Census U.S. Intercensal County population data, 1970-2014. Retrieved from https://www.nber.org/data/census-intercensal-county-population.html

USDA. (2018, February 21). Fertilizer use and price. Retrieved May 17, 2019, from https://www.ers.usda.gov/data-products/fertilizer-use-and-price.aspx

USDA National Agricultural Statistics Service. (2017). NASS-Quick Stats [Data set]. Retrieved from https://data.nal.usda.gov/dataset/nass-quick-stats

USDA National Agricultural Statistics Service Cropland Data Layer. (2010). Published crop-specific data layer [Online]. Retrieved from https://nassgeodata.gmu.edu/CropScape/

USDA-NASS. (2017). Census of Agriculture Retrieved from https://www.nass.usda.gov/AgCensus/index.php

Van Meter, K. J., & Basu, N. B. (2015). Signatures of human impact: Size distributions and spatial organization of wetlands in the prairie pothole landscape. *Ecological Applications: A Publication of the Ecological Society of America*, *25*(2), 451–465. https://doi.org/10.1890/14-0662.1

Van Meter, K. J., Basu, N. B., & Van Cappellen, P. (2017). Two centuries of nitrogen dynamics: Legacy sources and sinks in the Mississippi and Susquehanna River Basins. *Global Biogeochemical Cycles*, *31*, 2–3. https://doi.org/10.1002/2016gb005498

Van Meter, K. J., Basu, N. B., Veenstra, J. J., & Burras, C. L. (2016). The nitrogen legacy: Emerging evidence of nitrogen accumulation in anthropogenic landscapes. *Environmental Research Letters: ERL [Web Site]*, *11*, 035014. https://doi.org/10.1088/1748-9326/11/3/035014

Van Meter, K. J., Van Cappellen, P., & Basu, N. B. (2018). Legacy nitrogen may prevent achievement of water quality goals in the Gulf of Mexico. *Science*, *360*(6387), 427–430. https://doi.org/10.1126/science.aar4462

Waisanen, P. J., & Bliss, N. B. (2002). Changes in population and agricultural land in conterminous United States counties, 1790 to 1997. *Global Biogeochemical Cycles*, *16*(4), 1137. Retrieved from https://onlinelibrary.wiley.com/doi/pdf/10.1029/2001GB001843

Ward, M. H., Jones, R. R., Brender, J. D., de Kok, T. M., Weyer, P. J., Nolan, B. T., et al. (2018). Drinking water nitrate and human health: An updated review. *International Journal of Environmental Research and Public Health*, *15*, 1557. https://doi.org/10.3390/ijerph15071557

Yang, Q., Tian, H., Li, X., Ren, W., Zhang, B., Zhang, X., & Wolf, J. (2016). Spatiotemporal patterns of livestock manure nutrient production in the conterminous United States from 1930 to 2012. *The Science of the Total Environment*, *541*, 1592–1602. https://doi.org/10.1016/j.scitotenv.2015.10.044

Yiridoe, E. K., Voroney, R. P., & Weersink, A. (1997). Impact of alternative farm management practices on nitrogen pollution of groundwater: Evaluation and application of CENTURY model. *Journal of Environmental Quality*, *26*(5), 1255–1263. https://doi.org/10.2134/jeq1997.00472425002600050009x

Erratum

In the originally published version of this article, Figure 1 and its caption have a missing input label for fertilizer N. The error has been corrected to the online version of this article, but not the PDF, and the online version may be considered the authoritative version of record.

Figure 1.